Synthesis and crystal structure of Ru^{III}-supported tungstoantimonate [Sb$_2$W$_{20}$Ru$_2^{III}$(H$_2$O)$_2$(dmso)$_6$O$_{68}$]$^{4-}$

Li-Hua Bi *, Bao Li, Shuai Bi, Li-Xin Wu *

State Key Laboratory of Supramolecular Structure and Materials, College of Chemistry, Jilin University, Changchun 130012, PR China

ABSTRACT

The first Ru^{III}-supported tungstoantimonate [Ru^{II}(bpy)$_3$]$_2$[Sb$_2$W$_{20}$Ru$_2^{III}$(H$_2$O)$_2$(dmso)$_6$O$_{68}$] · 3dmso (bpy = bi-pyridine) (**1a**) has been successfully isolated as [Ru(bpy)$_3$]$^{2+}$ (Rubpy) salt by routine synthetic reaction in mixed solutions with dmso and water. Single-crystal X-ray analysis was carried out on **1a**, which crystallizes in the triclinic system space group *P*-1 with *a* = 16.804 (6), *b* = 16.988 (6), *c* = 17.666 (6) Å, α = 107.397 (13)°, β = 106.883 (13)°, γ = 103.616 (12)°. *V* = 4309 (3) Å^3, *Z* = 1 with *R*1 = 0.0773. The compound **1a** reveals the following features: (1) Rubpy is firstly used as an alternative ruthenium-source for the synthesis of Ru-substituted heteropolytungstate; (2) the structure of **1a** consists of four Ru^{III}–O–S(CH$_3$)$_2$ and two W–O–S(CH$_3$)$_2$ bonds resulting in an assembly with C_2 symmetry; (3) the Ru^{III} ions are linked to two dmso groups via two Ru^{III}–O–S(CH$_3$)$_2$ bonds, which represents the other dmso-coordination mode to Ru^{III} in POM chemistry. The cyclic voltammetry studies of **1a** in dmso/ H$_2$SO$_4$ (3/1 v/v) at pH 2.5 medium using the glassy carbon electrode as a working electrode show the respective electrochemical behaviors of the W-centers and the Ru-centers within **1a**, which could be separated clearly. In addition, the compound **1a** exhibits photoluminescence arising from π^*–t_{2g} ligand-to-metal transition of Rubpy.

© 2009 Elsevier Inc. All rights reserved.

1. Introduction

Polyoxometalates (POMs) represent a class of inorganic metal–oxygen clusters with an enormous structural and compositional variety and exciting properties, applications of which include catalysis, materials and medicine, etc. [1–3]. Transition-metal or noble-metal-substituted POMs are gaining widespread studies due to the possibility of tuning POM size, shape, charge density, acidity, redox potential, stability, and solubility characteristics as well as excellent catalytic properties [4–6]. In addition, the functionalities of POMs and their organic-inorganic hybrid materials are also a topic of continuing attention, owing to the potential of combining the characteristics of organic and inorganic components [7–10]. Therefore, the strong efforts for researchers are devoted to synthesize the POMs with multifunctionalities.

The noble metal ruthenium-substituted POMs are exploited rapidly recently because of the unique redox-active nature and catalytic properties of the element ruthenium [11–13]. In the last couple of years some researches have focused their studies on the catalytic properties of ruthenium-containing POMs and it has been proved that Ru-containing POMs have high reactivity and selectivity in the catalytic oxidation of a variety of organic

substrates by O$_2$ and H$_2$O$_2$ [14–16]. To date, several different Ru precursors, e.g. RuCl$_3$ · *n*H$_2$O, [Ru^{II}(H$_2$O)$_6$][C$_7$H$_7$SO$_3$]$_2$, Ru(acac)$_3$, *cis*-Ru(dmso)$_4$Cl$_2$, [Ru(*arene*)Cl$_2$]$_2$ (*arene* = benzene, *p*-cymene), etc. have been utilized to prepare Ru-containing POMs, resulting in some unexpected structural class of Ru-based POMs, such as [O{Ru^{IV}Cl(α_2-P$_2$W$_{17}$O$_{61}$)}$_2$]$^{16-}$ [17], [P$_2$W$_{17}$O$_{61}${Ru(C$_6$H$_6$)(H$_2$O)}]$^{8-}$ [18], [{PW$_{11}$O$_{39}${Ru(*arene*)}}$_2${WO$_2$}]$^{8-}$ [19], [{Ru(C$_6$H$_6$)(H$_2$O)} {Ru(C$_6$H$_6$)}(γ-XW$_{10}$O$_{36}$)]$^{4-}$ (X = Si, Ge) [20], [{Ru(C$_6$H$_6$)(H$_2$O)} {Ru(C$_6$H$_6$)}(XW$_9$O$_{34}$)]$^{4-}$ (X = Si, Ge) [21], [{K(H$_2$O)}$_3${Ru(*p*-cymene) (H$_2$O)}$_4$P$_8$W$_{49}$O$_{186}$(H$_2$O)$_2$]$^{27-}$ [22], [(PW$_9$O$_{34}$)$_2$(*cis*-WO$_2$)(*cis*-Ru$_2^{L^{Me}}$)]$^{13-}$ (*L^{Me}* = 1,3-dimethylimidazolidine-2-ylidene) [23], etc. However, the number of structurally fully-characterized ruthenium-POMs is still rather limited. Thus, the synthesis and structural characterization of new Ru-containing POMs by single crystal X-ray diffraction analysis is a great challenge and chance for their further application as catalyst.

The complex ruthenium (II) tris(bipyridine) (Rubpy) have attracted increasing attention due to its luminescence and electrochemistry properties. This compound has been employed as electrochemiluminescen (ECL) material for the solid-state ECL detection in capillary electrophoresis (CE) or CE microchip [24–26]. In recent years, much work has been contributed to the synthesis of hybrid materials combining POMs and Rubpy: McCormac et al. obtained the compound [Ru(bpy)$_3$]$_3$[P$_2$W$_{18}$O$_{62}$] and investigated its electrochemistry both in aqueous solution and solid state [27]; Keyes et al. prepared three compounds, [Ru(bpy)$_3$]$_{3.5}$[P$_2$W$_{17}$O$_{61}$(FeOH$_2$)], [Ru(bpy)$_3$]$_3$[P$_2$W$_{17}$O$_{61}$(FeBr)] and

$[Ru(bpy)_3]_5[P_2W_{17}O_{61}]$, and studied their photophysic properties [28]; Bond et al. showed the voltammetric, photo-physical and photo-electrochemical behaviors of the compounds $[Ru(bpy)_3]_2$ $[S_2M_{18}O_{62}]$ (M = Mo, W) [29]; Wang et al. reported on two compounds, $[Ru(bpy)_3]$–$[PMo_{12}O_{40}]$ and $[Ru(bpy)_3]_2[S_2Mo_{18}O_{62}]$ used as the bifunctional electrocatalyst for the fabrication of the chemically bulk-modified carbon paste electrode [30]. Recently, our group synthesized the nanoparticles of $[Ru(bpy)_3]_2$ $SiW_{12}O_{40} \cdot 2H_2O$ and applied them as electrochemiluminescence sensor [31]. However, all of the above compounds were characterized by elemental analysis, IR spectra and electrochemistry. To the best of our knowledge, there is only one report on the structurally characterized Rubpy-hybrid isopolytungstate $[Ru(bpy)_3]_2$ $[W_{10}O_{32}] \cdot 3dmso$ [32]. More recently, our group reported on the first crystal structure of Rubpy-hybrid heteropolytungstate $[Ru(bpy)_3]_4[Sb_2W_{20}(OH)_2(dmso)_2O_{66}] \cdot 16dmso \cdot 2H_2O$ [33].

As a part of continuing work, here we report on the synthesis, characterization and crystal structure of other Ru^{III}-substituted and dmso-coordinated tungstoantimonate $[Ru^{II}(bpy)_3]_2[Sb_2W_{20}$ $Ru_2^{III}(H_2O)_2(dmso)_6O_{68}] \cdot 3dmso$ (**1a**). Interestingly, (i) Rubpy unit was demonstrated as an alternative ruthenium-source to synthesize Ru^{III}-substituted POM; (ii) in **1a**, the dmso groups are coordinated to the Ru^{III} centers via the oxygen atoms, which are different from the previously reported $Ru(dmso)_3$-supported POMs, such as $[HW_9O_{33}Ru_2^{II}(dmso)_6]^{7-}$ [34], $[Ru^{II}(dmso)_3(H_2O)XW_{11}O_{39}]^{6-}$ (X = Ge, Si) [35], $[HXW_7O_{28}Ru^{II}(dmso)_3]^{6-}$ (X = P, As) [36].

2. Experimental section

2.1. Materials and methods

All chemicals were commercially purchased and used without further purification. $K_6Na_4[Mn_2(H_2O)_6(WO_2)_2(\beta\text{-}SbW_9O_{33})_2]$ was synthesized according to the literature [37,38] and characterized by IR spectrum. The elemental analyses of Ru, Sb, and W were carried out by means of an ICP-AES analyzer. The elemental analyses of N, S, C and H were performed on a Perkin-Elmer 2400 CHN elemental analyzer. The IR spectra were recorded on a Bruker IFS66 V FT-IR spectrometer equipped with a DGTS detector (32 scans) using KBr pellets. The thermal gravimetric analysis (TGA) was carried out on a TGA Q500 V20.8 Build 34 thermal analysis system. Electrochemical measurements were carried out on CHI 660C electrochemical workstation at room temperature under nitrogen atmosphere. A three electrode electrochemical cell was used with a glassy carbon electrode (GCE) as the working electrode, a platinum wire as the counter and an Ag/AgCl as reference electrode. Luminescent measurements were performed on a HITACHI F-4500 Fluorescence spectrophotometer.

2.2. Synthesis of $[Ru^{II}(bpy)_3]_2[Sb_2W_{20}Ru_2^{III}(H_2O)_2(dmso)_6O_{68}] \cdot 3dmso$ (**1a**)

The compound **1a** was synthesized by addition of 0.6 g (0.8 mmol) $Ru(bpy)_3Cl_2$ followed by 1.1 g (0.2 mmol) $K_6Na_4[Sb_2$ $W_{20}Mn_2(H_2O)_6O_{70}]$ in 20 mL dmso/H_2O (v:v = 1:1). The solution was heated to 80 °C for 1 h. The solution was filtered after it had cooled. Single crystals suitable for X-ray analysis were obtained by slow evaporation of the filtrate at room temperature. Yield: 0.45 g (32% based on $K_6Na_4[Sb_2W_{20}Mn_2(H_2O)_6O_{70}]$). Anal. Calcd (Found) for **1a**: Ru 5.7 (5.4), Sb 3.4 (3.3), W 51.9 (50.9), N 2.4 (2.5), S 4.1 (3.6), C 13.2 (12.6), H 1.5 (1.7). IR (ν_{max}/cm^{-1}): 1466m, 1445m, 1425m, 1310w, 1271w, 1242w, 1163w, 1121w, 1070w, 1032w, 962m, 876sh, 858m, 814s, 755sh, 744s, 729sh, 661sh, 611sh, 522w, 466w, 430m.

Empirical formula	$C_{78}H_{106}N_{12}O_{79}Ru_4S_9Sb_2W_{20}$	
Formula weight	7089.07	
Temperature	293(2) K	
Wavelength	0.71073 Å	
Crystal system	Triclinic	
Space group	$P-1$	
Unit cell dimensions	$a = 16.804(6)$ Å	$\alpha = 107.397(13)$.
	$b = 16.988(6)$ Å	$\beta = 106.883(13)$.
	$c = 17.666(6)$ Å	$\gamma = 103.616(12)$.
Volume	4309 (3) Å^3	
Z	1	
Density (calculated)	2.732 Mg/m^3	
Absorption coefficient	14.119 mm^{-1}	
F(000)	3192	
Data/restraints/parameters	18036/20/882	
Goodness-of-fit on F^2	1.047	
Final R indices [$I > 2$sigma(I)]	^{a}$R1 = 0.0773$, ^{b}$wR2 = 0.1814$	
R indices (all data)	^{a}$R1 = 0.1431$, ^{b}$wR2 = 0.2220$	

^{a} $R_1 = (\Sigma|F_o| - |F_c|)/(\Sigma|F_c|)$.
^{b} $wR_2 = \Sigma[w(F_o^2 - F_c^2)^2]/\Sigma[w(F_o^2)^2]^{1/2}$.

2.3. X-ray crystallography

X-ray single-crystal data for **1a** was set on the end of a glass capillary for indexing and intensity data collection at 293 K on the a Rigaku R-AXIS RAPID IP diffractometer with graphite monochromated Mo$K\alpha$ radiation ($\lambda = 0.71073$ Å). Direct method was used to solve the structure and to locate the heavy atoms (SHELXS97). Then the remaining atoms were found from successive difference maps (SHELXL97). Further details of the X-ray structural analysis are given in Table 1. Selected bond lengths and angles are listed in Table 2.

3. Results and discussion

3.1. Synthesis

Synthesis of **1a** was accomplished by the reaction of Rubpy and $[Sb_2W_{20}Mn_2(H_2O)_6O_{70}]^{10-}$ in mixed media with dmso/H_2O (v:v = 1:1). In order to identify the crucial components/conditions for the formation of **1a** we modified the reaction conditions systematically. For example, we tested if **1a** can also be synthesized using Mn-analogues, such as $[Sb_2W_{20}Ni_2(H_2O)_6O_{70}]^{10-}$, $[Sb_2W_{20}Fe_2$ $(H_2O)_6O_{70}]^{8-}$, $[Sb_2W_{22}(OH)_2O_{74}]^{12-}$ substituting for $[Sb_2W_{20}Mn_2$ $(H_2O)_6O_{70}]^{10-}$ in the presence of Rubpy. Interestingly, three different dmso-coordinated tungstoantimonate were obtained, one of which has been published [33], and other two compounds will be published elsewhere. Also we tested a two-step procedure: (i) reaction of $[Sb_2W_{20}Mn_2(H_2O)_6O_{70}]^{10-}$ with Rubpy and isolation of $[Ru(bpy)_3]$–$[Sb_2W_{20}Mn_2(H_2O)_6O_{70}]$ (**1b**); (ii) redissolution of **1b** in dmso/H_2O with heating. This time we obtained **1a** as based on IR. These observations allow the conclusion that the presence of $[Sb_2W_{20}Mn_2(H_2O)_6O_{70}]^{10-}$ and Rubpy is crucial for the formation of **1a**. Therefore, the formation mechanism of **1a** involves the decomposition of Rubpy, coordination of dmso and substitution of manganese.

3.2. Crystal structure

The structure of **1a** was solved in the triclinic system space group $P-1$, and it consists of two trilacunary species of (β-B–SbW_9O_{33}) linked by two WO(dmso) groups and two $Ru(H_2O)(dmso)_2$ units, leading to a unprecedented

Table 2
Selected bond lengths (Å) and angles (°) for $[Ru^{II}(bpy)_3]_2[Sb_2W_{20}Ru_2^{III}(H_2O)_2(dmso)_6O_{68}] \cdot 3dmso$ (**1a**).

Ru1–N1	2.08 (2)	Ru1–N2	2.03 (2)
Ru1–N3	2.01 (2)	Ru1–N4	2.06 (3)
Ru1–N5	2.04 (2)	Ru1–N6	1.98 (19)
Ru2–O2	2.12 (17)	Ru2–O17	2.21 (16)
Ru2–O27	2.05 (15)	Ru2–O35	2.01 (2)
Ru2–O36	2.01 (2)	Ru2–O37	2.19 (2)
Sb1–O16	2.01 (14)	Sb1–O6	1.97 (15)
Sb1–O25	2.00 (15)	W10–O19	1.80 (16)
W10–O31	1.95 (16)	W10–O34	2.20 (15)
W10–O38	2.10 (17)	W10–O32	1.72 (15)
W10–O33	1.92 (15)	S2–O38	1.52(19)
S1–O37	1.60 (2)	S3–O36	1.55 (4)
O32–W10–O19	101.3 (8)	O32–W10–O33	96.7 (7)
O38–W10–O34	82.0 (6)	O31–W10–O34	81.0 (6)
O33–W10–O34	82.2 (6)	O19–W10–O34	85.3 (6)
O32–W10–O34	173.4 (8)	O31–W10–O38	81.9 (7)
O33–W10–O38	81.8 (7)	O19–W10–O38	167.2 (6)
O32–W10–O38	91.4 (8)	O33–W10–O31	158.0 (7)
O19–W10–O31	94.5 (7)	O32–W10–O31	98.4 (7)
O19–W10–O33	98.2 (7)	O6–Sb1–O16	92.2 (7)
O6–Sb1–O25	89.4 (6)	O25–Sb1–O16	91.2 (6)
O35–Ru2–O36	86.3 (9)	O35–Ru2–O27	96.9 (7)
O36–Ru2–O27	94.4 (8)	O35–Ru2–O2	98.3 (8)
O36–Ru2–O2	175.3 (8)	O27–Ru2–O2	86.1 (7)
O35–Ru2–O37	88.9 (9)	O36–Ru2–O37	92.3 (9)
O37–Ru2–O17	86.6 (8)	O2–Ru2–O17	88.0 (7)
O27–Ru2–O17	88.4 (6)	O36–Ru2–O17	87.3 (8)
O35–Ru2–O17	172.0 (8)	O2–Ru2–O37	86.9 (8)
O27–Ru2–O37	171.4 (9)		
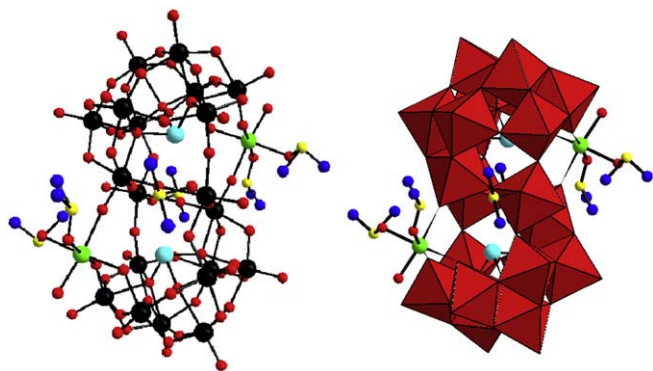
Fig. 1. Ball and stick (left) and polyhedral (right) representation of the polyoxoanion **1**. The balls represent tungsten (black), antimony (cyan), ruthenium (green), oxygen (red), sulfur (yellow), and carbon (blue). The WO_6 octahedra are red. No hydrogens shown for clarity. (For interpretation of the references to colour in this figure legend, the reader is referred to the web version of this article.)

Ru^{III}-substituted sandwich-type tungstoantimonate attached by six *dmso* groups (Fig. 1). Four of the six dmso groups are coordinated to the two Ru centers via $Ru–O–S(CH_3)_2$ bonds and the other two dmso ligands are bound to the two W centers linking the $(\beta$-B–SbW_9O_{33})$ units via $W–O–S(CH_3)_2$ bonds. Bonding of dmso the tungsten atom of a polyoxoanion has been recently reported by our group [33].

In 1997, Krebs et al. had firstly described the structural type of $[Sb_2W_{22}O_{74}(HO)_2]^{12-}$, which is composed of two identical $(\beta$-B–SbW_9O_{33})$ fragments joined together by four WO_6 octahedra, among which the two external ones display a facial $\{WO_2(OH)\}^+$ arrangement [37,38]. Subsequently, the same authors showed that the two fac-$\{WO_2(OH)\}^+$ groups can be replaced by various $M^{n+}(H_2O)_3$ units forming transition metal substituted derivatives $[M_2(H_2O)_6(WO_2)_2(\beta$-SbW_9O_{33})_2]^{(14-2n)-}$ (M^{n+} = Fe^{3+}, Co^{2+}, Mn^{2+}, Ni^{2+}, Cu^{2+}, Zn^{2+}) [37,38]. Recently, Proust reported the organo-Ru

moieties replaced two fac-$\{WO_2(OH)\}^+$ fragments resulting in the tungstoantimonate $[Sb_2W_{20}O_{70}\{Ru(p\text{-}cymene)\}_2]^{10-}$ [39]. More recently, our group presented the V^{IV}-substituted tungstoantimonate $[Sb_2W_{20}(VO)_2(H_2O)_4O_{70}]^{10-}$ [40] and one-dimensional chain-like Cd^{II}-substituted tungstoantimonate $[Sb_2W_{21}Cd(OH)_2O_{73}]^{14-}$ [41].

The structure of the polyanion $[Sb_2W_{20}Ru_2^{III}(H_2O)_2(dmso)_6O_{68}]^{4-}$ (**1**) is closely related to $[Sb_2W_{22}O_{74}(OH)_2]^{12-}$. Therefore, polyanion **1** can be described as that two $\{Ru(H_2O)(dmso)_2\}$ species replace the two fac-$\{WO_2(OH)\}^+$ moieties and two dmso groups are coordinated to two tungsten atoms in the polyanion fragment. Both Ru centers in **1** are coordinated by six oxo ligands, which include three μ_2-oxo-groups from the tungsten-oxo framework, two oxo-groups from the terminal dmso ligands and one from the coordinated water molecule (Fig. 2). The Ru2–O bond lengths are in the expected range of around 2.01–2.20 Å [Ru2–O(W), 2.05–2.20 Å; Ru2–O(S), 2.01–2.19 Å; Ru2–O(water), 2.01 Å]. In addition, W10 is coordinated to four bridging oxo-groups from the tungsten-oxo framework, to one oxygen atom from the terminal dmso ligand and to one terminal oxygen atom. The W10–O bond lengths are also in the expected range of around 1.72–2.20 Å [W10–O(W), 1.80–2.20 Å; W10–O(S), 2.10 Å; W10–O(terminal), 1.72 Å]. It can be seen that in $\{Ru(H_2O)(dmso)_2\}$ units DMSO molecules are coordinated to Ru ions via Ru–O bonds, not bound via Ru–S bonds. Such bonding mode is different from previously reported $Ru(dmso)_3$-supported POMs (see Fig. 3) [34–36].

Recently, same author reported three $Ru(dmso)_3$-supported POMs: the first one is two $Ru(dmso)_3$ units-supported isopolytungstate $[HW_9O_{33}Ru_2^{II}(dmso)_6]^{7-}$ (**2**), which is composed of a nonatungstate wheel stabilized by two $Ru(dmso)_3$ groups, representing a class of isopolyanions supporting photochromic moieties [34]; The second one is one $Ru(dmso)_3$ unit-supported monolacunary tungstosilicate and tungstogermanate $[Ru(dmso)_3(H_2O)XW_{11}O_{39}]^{6-}$ (X = Ge, Si) (**3**), which consist of a $Ru(dmso)_3(H_2O)$ unit linked to a monolacunary $[XW_{11}O_{39}]^{8-}$ (X = Ge, Si) Keggin fragment via two Ru–O–W bonds resulting in an assembly with C_1 symmetry [35]; the third one is one $Ru(dmso)_3$ unit-supported tungstoarsenate and tungstophosphate $[HXW_7O_{28}Ru(dmso)_3]^{6-}$ (X = P, As) (**4**), which are composed of a $Ru(dmso)_3$ group attached to an unprecedented heptatungstate fragment via two Ru–O–W bonds and one Ru–O–X bond representing a fundamentally novel mode of Ru-coordination to a polyanion framework [36]. As shown in Fig. 3, it can be seen that the $Ru(dmso)_3$ units are bound to the polyanion fragment via Ru–S(O) bonds in above three compounds although the $Ru(dmso)_3$ units have different coordination modes to the different tungsten-oxo species. However, in our case of **1**, the only two dmso groups are coordinated to the Ru centers via Ru–O(S) bonds. Such bonding model was observed in organic-Ru complex [42], however, it has never been seen in $\{Ru(dmso)\}$-supported POMs. The reason for the different coordination mode of ligands dmso to the Ru centers is most likely due to the use of the different Ru-precursor during the synthesis of compounds **1–4**, for example, $Ru(dmso)_4Cl_2$ was used as precursor for the synthesis of compounds **2–4**, however, Rubpy was utilized for the preparation of compound **1**.

Bond valence sum calculations [43] indicate that the oxidation state of the Ru coordinated to the polyanion framework is +3, and there are no other protonation sites on **1** except that the water molecules are coordinated to the Ru centers, therefore, the charge of the polyanion **1** must be −4. In the solid state, the negative charge of **1** is balanced by two $[Ru(bpy)_3]^{2+}$ cations, located by X-ray diffraction. Elemental analyses of **1a** further confirmed the chemical composition. In addition, thermogravimetric analysis allowed us to estimate the number of water molecules, dmso molecules including all noncoordinated and coordinated ones and 2,2′-bipyridyl ligands to ruthenium.
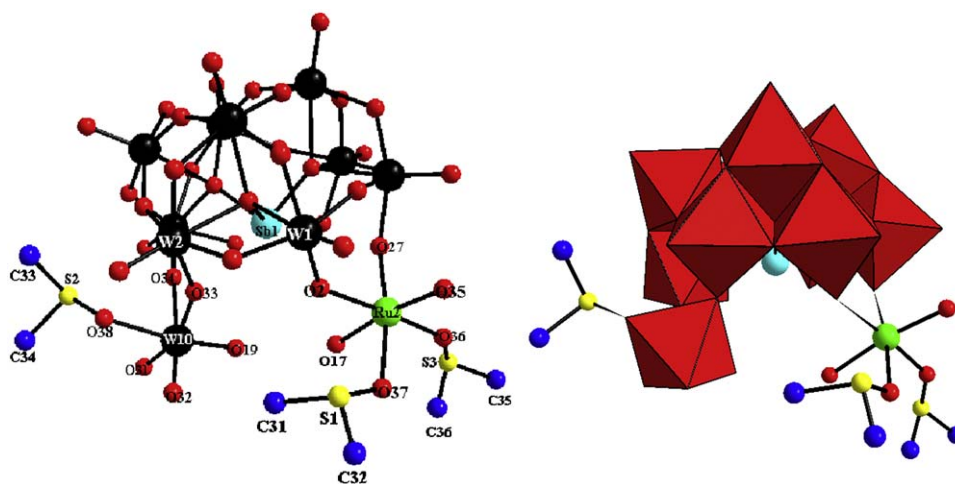
Fig. 2. Ball-and-stick (left) and combined polyhedral/ball-and-stick (right) representation of the asymmetric unit of **1** with atom labeling. The color codes are the same as in Fig. 1. Hydrogen atoms have been omitted for clarity.
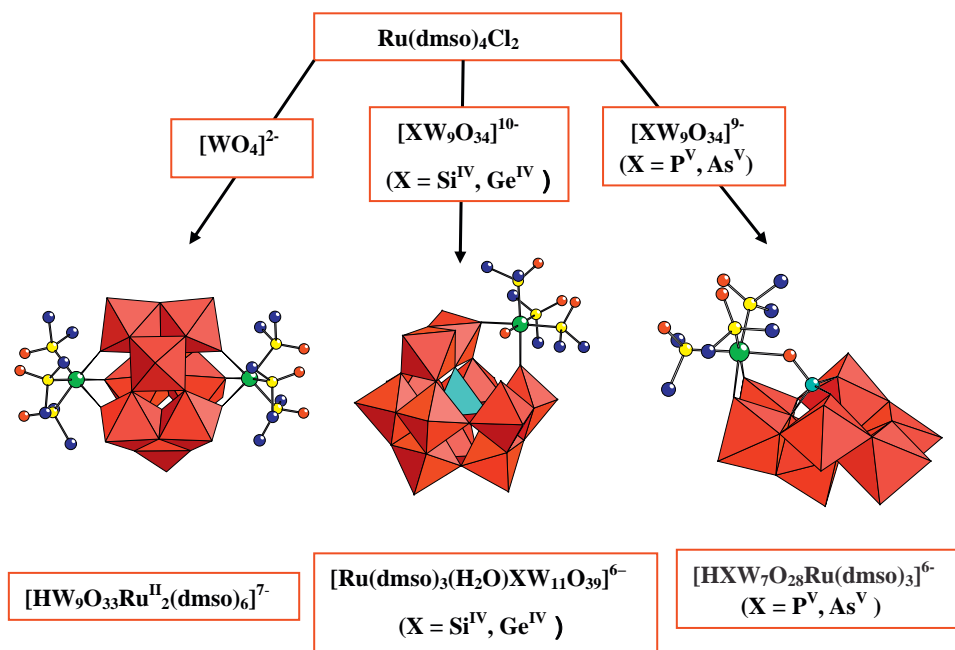

Fig. 3. Polyhedral representation of $[HW_9O_{33}Ru^{II}_2(dmso)_6]^{7-}$ (**2**), $[Ru(dmso)_3(H_2O)XW_{11}O_{39}]^{6-}$ ($X = Ge$, Si) (**3**), $[HXW_7O_{28}Ru(dmso)_3]^{6-}$ ($X = P$, As) (**4**). The balls represent ruthenium (green), oxygen (red), sulfur (yellow), phosphorous/arsenic (cyan), and carbon (blue). The SiO_4/GeO_4 tetrahedra are cyan and the WO_6 octahedra are red. No hydrogens shown for clarity. (For interpretation of the references to colour in this figure legend, the reader is referred to the web version of this article.)

The title polyanion was isolated as its tris-bipyridine-ruthenium(II) salt, $[Ru(bpy)_3]_2[Sb_2W_{20}Ru_2(H_2O)_2(dmso)_6O_{68}]\cdot$ 3dmso (**1a**). We have characterized **1a** in solid state by IR, TGA and elemental analysis, in solution by electrochemistry, and we also studied its luminescence.

3.3. IR spectrum

As expected, the IR spectrum of **1a** (see Supp. Info, Figures SI1) is very similar to that of $[Sb_2W_{20}Mn_2(H_2O)_6O_{70}]^{10-}$ and $Ru(bpy)_3$ Cl_2 superimposed on each other, except that some bands are slightly shifted. This implies that the tungsten-oxo framework and Rubpy units are maintained in **1a**. In addition, the IR spectrum of **1a** shows the expected S–O stretching vibrations of dmso at 1121, 1070, and 1032 cm^{-1} [44].

3.4. Thermal analysis

Thermal gravimetric analysis has been performed for **1a** between 20 and 800 °C. The compound **1a** shows a continuous weight-loss process (see Fig. 4), which corresponds to the removal of coordinated water molecules, dmso molecules including all noncoordinated and coordinated ones, and 2, 2′-bipyridyl ligands to ruthenium. The thermal gravimetric (TG) curve of **1a** shows the total weight loss of ca. 23.6% in the measurement range (calcd ca. 23.6%). Thus, it can be seen that the total weight losses are completely consistent with the calculated values.

3.5. Electrochemistry

Cyclic voltammetry (CV) studies of **1a** were performed in dmso with H_2SO_4 at pH 2.5 in the potential range from −0.6 to 1.4 V.

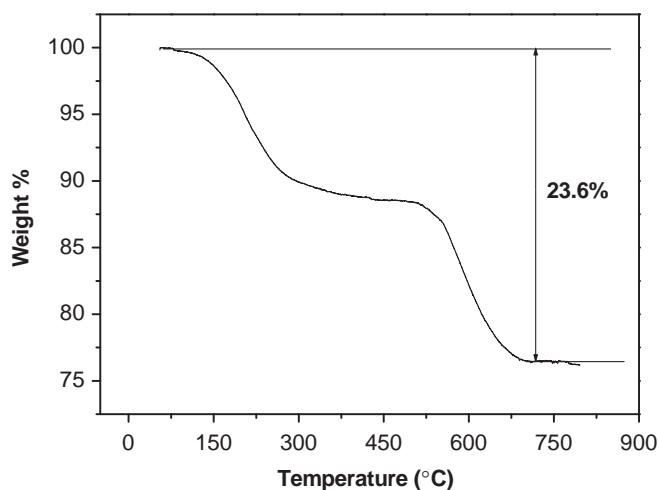Fig. 4. TGA curve of $[Ru^{II}(bpy)_3]_2[Sb_2W_{20}Ru_2^{III}(H_2O)_2(dmso)_6O_{68}] \cdot 3dmso$ (1a).
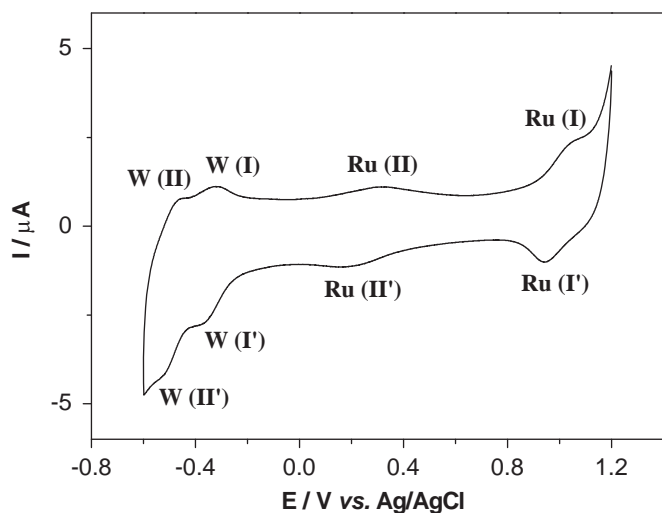

Fig. 5. Cyclic voltammogram of 0.5 mM 1a in dmso+H_2SO_4 at pH 2.5 at a bare GCE with scan rate 100 mV s^{-1}.

The cyclic voltammogram of 1a displays four redox waves at +1.00, 0.24, −0.35 and −0.49 V, as shown in Fig. 5. The first wave is a one-electron process, assigned to the $Ru^{3+/2+}$ couple originating from Rubpy; the second wave is also one-electron process, assigned to the $Ru^{4+/3+}$ couple originating from Ru centers coordinated to the tungsten-oxo fragment, while the latter two waves are multi-electron processes attributed to the reduction of the tungstoantimonate(III) framework, which are similar to ones of $[V_2(H_2O)_6(WO_2)_2(\beta\text{-}SbW_9O_{33})_2]^{6-}$ and $[Fe_2(H_2O)_6(WO_2)_2(\beta\text{-}SbW_9O_{33})_2]^{8-}$ reported by the same authors [40,45]. The CVs of 1a in same pH medium at different scan rates are shown in Fig. 6a. The peak currents of 1a are linearly proportional to the scan rates, taking the redox peaks of Ru (II) and W (I) in 1a as representative, as shown in Fig. 6b and c. This indicates that the redox reactions exhibit surface processes.

3.6. Luminescent property

The luminescent property of Rubpy complex has been extensively investigated, however, studies of Rubpy-containing POMs are limited. Keyes et al. prepared three compounds, $[Ru(bpy)_3]_{3.5}[P_2W_{17}O_{61}(FeOH_2)]$, $[Ru(bpy)_3]_3[P_2W_{17}O_{61}(FeBr)]$
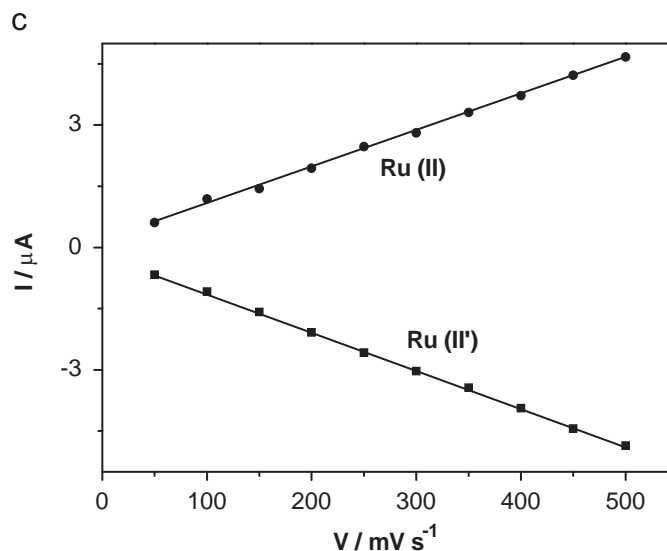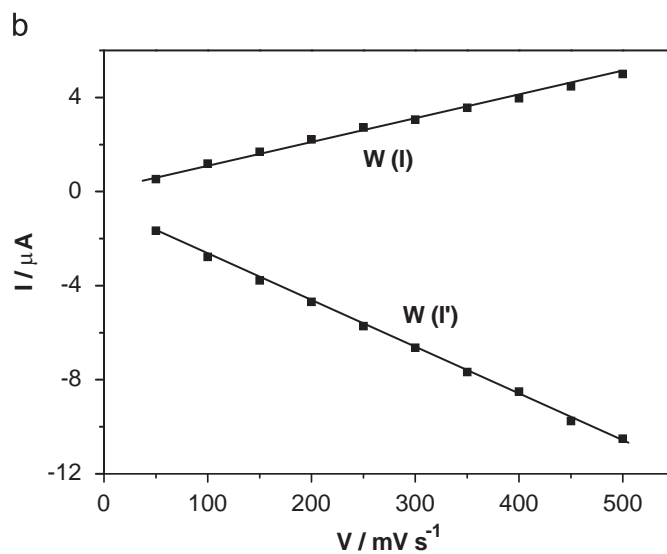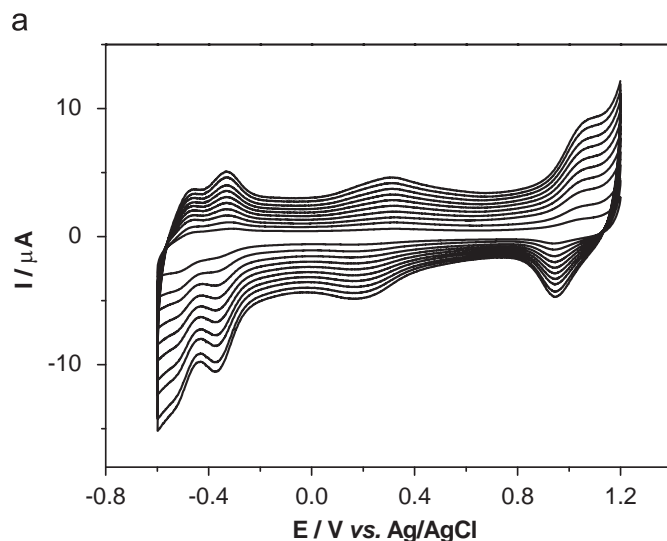

Fig. 6. (a) Cyclic voltammograms of 1a in a pH 2.5 medium (dmso+H_2SO_4) at scan rates of 50, 100, 150, 200, 250, 300, 350, 400, 450, and 500 mV s^{-1}; (b) shows the relationship of the scan rates vs. the oxidation peak currents of W (I) and reduction peak currents of W (I′); (c) shows the relationship of the scan rates vs. the oxidation peak currents of Ru (II) and reduction peak currents of Ru (II′). Polyanion concentration: 0.5 mM. The working electrode was glassy carbon, and the reference electrode was Ag/AgCl.

Fig. 7. Excitation spectrum of compound **1a** (8.9×10^{-8} M) at 605 nm in DMSO/H_2O.

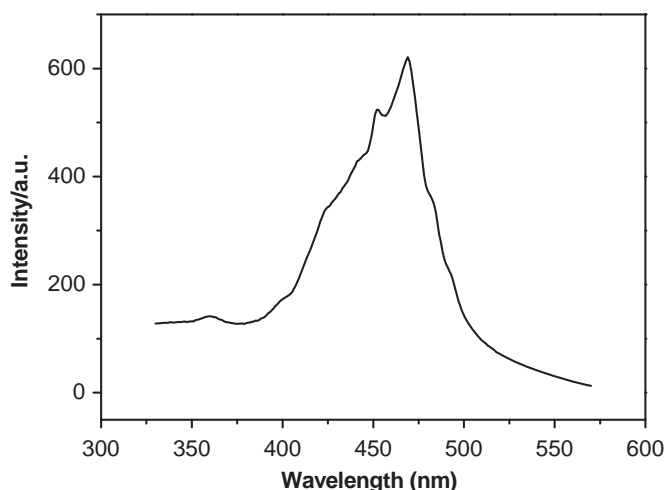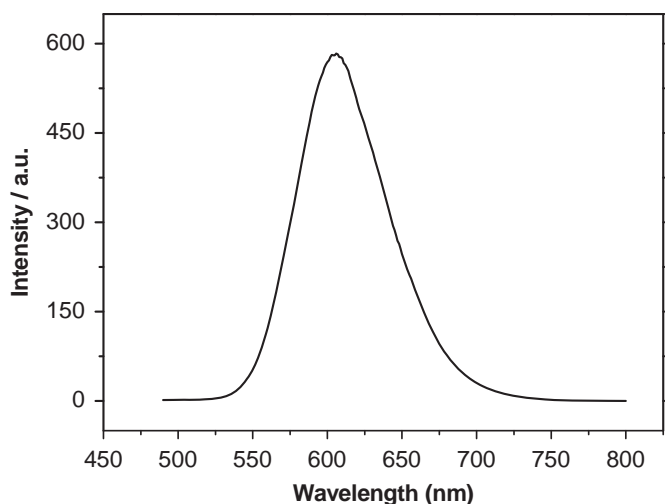**Fig. 8.** Emission spectrum of compound **1a** (8.9×10^{-8} M) at 469 nm in DMSO/H_2O.

and $[Ru(bpy)_3]_5[P_2W_{17}O_{61}]$, and studied their photophysic properties [28]; Bond et al. reported on photo-physical and photo-electrochemical behaviors of the compounds $[Ru(bpy)_3]_2$ $[S_2M_{18}O_{62}]$(M = Mo, W) [29]. In our work, photoluminescent property of compound **1a** was investigated in the mixed medium with dmso and water at room temperature. The excitation spectrum of **1a** was showed in Fig. 7. It can be seen that the spectrum has the most intense band at ca. 469 nm assigned to the singlet metal-to-ligand (MLCT) $d-\pi^*$ transitions, which is also visible for pure Rubpy (see Supp. Info, Figures SI2), indicating that the photoluminescent property of Rubpy is retained in compound **1a**. The emission spectrum of **1a** is showed in Fig. 8, excited at 469 nm. The emission spectrum for **1a** is quite similar to that of Rubpy (see Supp. Info, Figures SI3) and it shows a characteristic broad band, originating from π^*-t_{2g} ligand-to-metal transition of Rubpy.

4. Conclusions

In conclusion, we synthesized the first tri-bipyridine-ruthenium(II) salt of di-ruthenium(III)-containing tungstoantimonate $[Ru^{II}(bpy)_3]_2[Sb_2W_{20}Ru_2^{III}(H_2O)_2(dmso)_6O_{68}] \cdot 3dmso$ (**1a**).

The compound **1a** is of interest for several reasons: (i) Rubpy is firstly used as an alternative ruthenium-source to prepare the Ru-substituted POM; (ii) **1a** represents the first example of Ru(dmso)-supported sandwich-type tungstoantimonate; (iii) **1a** is unusual as it not only contains dmso molecules coordinated to Ru(III) centers but also to W(VI) centers via Ru(W)–O–S(CH₃)₂ bonds; (iv) **1a** adds the new member to organo-Ru containing POMs and substituted-type tungstoantimonate in particular; (v) The electro-chemical behaviors of the compound **1a** showed the expected redox couples of the Ru and W atoms in the mixed medium of DMSO/H_2SO_4 at pH 2.5; (vi) The compound **1a** exhibited photoluminescence originating from π^*-t_{2g} ligand-to-metal transition of Rubpy; (vii) The structure of **1a** allows for a multitude of studies including organic catalysis, multifunctional electrocatalyst and solid-state ECL detection. Some of this work is currently in progress, and the results will be reported in due time.

Supporting Information Available: Fourier transform IR spectra of **1a**, Rubpy and $K_6Na_4[Mn_2(H_2O)_6(WO_2)_2(\beta\text{-}SbW_9O_{33})_2]$. Excitation and emission spectra of Rubpy in H_2O. X-ray crystallographic data of **1a** in CIF format.

Appendix A. Supplementary data

Supplementary data associated with this article can be found in the online version at doi:10.1016/j.jssc.2009.03.009.

References

[1] C.L. Hill, Chem. Rev., 98, 1998, p. 1, (special thematic issue on polyoxometa-lates).
[2] J.J. Borrás-Almenar, E. Coronado, A. Müller, M.T. Pope (Eds.), Polyoxometalate Molecular Science, Kluwer, Dordrecht, The Netherlands, 2004.
[3] D.L. Long, E. Burkholder, L. Cronin, Chem. Soc. Rev. 36 (2007) 105.
[4] [a] L.H. Bi, U. Kortz, B. Keita, L. Nadjo, H. Borrmann, Inorg. Chem. 43 (2004) 8367;
[b] L.H. Bi, M. Reicke, U. Kortz, B. Keita, L. Nadjo, R.J. Clark, Inorg. Chem. 43 (2004) 3915;
[c] L.H. Bi, U. Kortz, B. Keita, L. Nadjo, L. Daniels, Eur. J. Inorg. Chem. 15 (2005) 3034.
[5] [a] S.T. Zheng, J. Zhang, G.Y. Yang, Angew. Chem. Int. Ed. 47 (2008) 3909;
[b] J.W. Zhao, J. Zhang, S.T. Zheng, G.Y. Yang, Chem. Commun. (2008) 570;
[c] B. Li, L.H. Bi, W. Li, L.X. Wu, J. Solid State Chem. 181 (2008) 3337.
[6] [a] Z. Luo, P. Kogerler, R. Cao, I. Hakim, C.L. Hill, Dalton Trans. 1 (2008) 54;
[b] B. Botar, P. Kogerler, C.L. Hill, Inorg. Chem. 46 (2007) 5398;
[c] Z.M. Zhang, S. Yao, E.B. Wang, C. Qin, Y.F. Qi, Y.G. Li, R. Clerac, J. Solid State Chem. 181 (2008) 715.
[7] [a] G.G. Gao, F.Y. Li, L. Xu, X.Z. Liu, Y.Y. Yang, J. Am. Chem. Soc. 130 (2008) 10838;
[b] J.P. Wang, S.Z. Li, Y. Shen, J.Y. Niu, Cryst. Growth Des. 8 (2008) 372.
[8] [a] C.I. Ritchie, C. Streb, J. Thiel, S.G. Mitchell, H.N. Miras, D.L. Long, T. Boyd, R.D. Peacock, T. McGlone, L. Cronin, Angew. Chem. Int. Ed. 47 (2008) 6881;
[b] C.P. Pradeep, D.L. Long, G.N. Newton, Y.F. Song, L. Cronin, Angew. Chem. Int. Ed. 47 (2008) 4388;
[c] Y.F. Song, N. McMillan, D.L. Long, J. Thiel, Y.L. Ding, H.S. Chen, N. Gadegaard, L. Cronin, Chem. A Eur. J. 14 (2008) 2349;
[d] J.M. Breen, W. Schmitt, Angew. Chem. Int. Ed. 47 (2008) 6904.
[9] [a] J.W. Zhao, H.P. Jia, J. Zhang, S.T. Zheng, G.Y. Yang, Chem. A Eur. J. 13 (2007) 10030;
[b] X.Y. Zhao, D.D. Liang, S.X. Liu, C.Y. Sun, R.G. Cao, C.Y. Gao, Y.H. Ren, Z.M. Su, Inorg. Chem. 47 (2008) 7133;
[c] A.X. Tian, J. Ying, J. Peng, J.Q. Sha, Z.G. Han, J.F. Ma, Z.M. Su, N.H. Hu, H.Q. Jia, Inorg. Chem. 47 (2008) 3274.
[10] [a] H. Liu, C. Qin, Y.G. Wei, L. Xu, G.G. Gao, F.Y. Li, X.S. Qu, Inorg. Chem. 47 (2008) 4166;
[b] J. Hao, Y. Xia, L.S. Wang, L. Ruhlmann, Y.L. Zhu, Q. Li, P.C. Yin, Y.G. Wei, H.Y. Guo, Angew. Chem. Int. Ed. 47 (2008) 2626;
[c] L.H. Bi, B. Li, L.X. Wu, K.Z. Shao, Z.M. Su, J. Solid State Chem. 182 (2009) 83.
[11] T. Naota, H. Takaya, S.I. Murahashi, Chem. Rev. 98 (1998) 2599.
[12] R. Neumann, M. Dahan, J. Am. Chem. Soc. 120 (1998) 11969.
[13] R. Neumann, M. Dahan, Nature 388 (1997) 353.
[14] R. Neumann, A.M. Khenkin, M. Dahan, Angew. Chem. Int. Ed. Engl. 34 (1995) 1587.
[15] C.L. Hill, C.M. Prosser-McCartha, Coord. Chem. Rev. 143 (1995) 407.
[16] C.N. Kato, A. Shinohara, N. Moriya, K. Nomiya, Catal. Commun. 7 (2006) 413.

[17] W.J. Randall, T.J.R. Weakley, R.G. Finke, Inorg. Chem. 32 (1993) 1068.
[18] Y. Sakai, A. Shinohara, K. Hayashi, K. Nomiya, Eur. J. Inorg. Chem. 1 (2006) 163.
[19] V. Artero, D. Laurencin, R. Villanneau, R. Thouvenot, P. Herson, P. Gouzerh, A. Proust, Inorg. Chem. 44 (2005) 2826.
[20] L.H. Bi, U. Kortz, M.H. Dickman, B. Keita, L. Nadjo, Inorg. Chem. 44 (2005) 7485.
[21] L.H. Bi, E.V. Chubarova, N.H. Nsouli, M.H. Dickman, U. Kortz, B. Keita, L. Nadjo, Inorg. Chem. 45 (2006) 8575.
[22] S.S. Mal, N.H. Nsouli, M.H. Dickman, U. Kortz, Dalton Trans. 25 (2007) 2627.
[23] V. Artero, A. Proust, P. Herson, F. Villain, C.C.D. Moulin, P. Gouzerh, J. Am. Chem. Soc. 125 (2003) 11156.
[24] M.M. Richter, Chem. Rev. 104 (2004) 3003.
[25] A. Arora, J.C.T. Eijkel, W.E. Morf, A. Manz, Anal. Chem. 73 (2001) 3282.
[26] X.P. Sun, Y. Du, L.X. Zhang, S.J. Dong, E.K. Wang, Anal. Chem. 79 (2007) 2588.
[27] N. Fay, E. Dempsey, A. Kennedy, T. McCormac, J. Electroanal. Chem. 556 (2003) 63.
[28] M.K. Seery, N. Fay, T. McCormac, E. Dempsey, R.J. Forster, T.E. Keyes, Phys. Chem. Chem. Phys. 7 (2005) 3426.
[29] N. Fay, V.M. Hultgren, A.G. Wedd, T.E. Keyes, R.J. Forster, D. Leane, A.M. Bond, Dalton Trans. 35 (2006) 4218.
[30] [a] X.L. Wang, Q. Zhang, Z.B. Han, E.B. Wang, Y.Q. Guo, C.W. Hu, J. Electroanal. Chem. 563 (2004) 221;

[b] X.L. Wang, Z.B. Han, E.B. Wang, H. Zhang, C.W. Hu, Electroanalysis 15 (2003) 1460.
[31] L.H. Bi, W.H. Zhou, H.Y. Wang, S.J. Dong, Electroanalysis 20 (2008) 996.
[32] Z.B. Han, E.B. Wang, G.Y. Luan, Y.G. Li, C.W. Hu, P. Wang, N.H. Hu, H.Q. Jia, Inorg. Chem. Commun. 4 (2001) 427.
[33] L.H. Bi, B. Li, L.X. Wu, Inorg. Chem. Commun. 11 (2008) 1187.
[34] L.H. Bi, F. Hussain, U. Kortz, M. Sadakane, M.H. Dickman, Chem. Commun. (2004) 1420.
[35] L.H. Bi, U. Kortz, B. Keita, L. Nadjo, Dalton Trans. (2004) 3184.
[36] L.H. Bi, M.H. Dickman, U. Kortz, I. Dix, Chem. Commun. (2005) 3962.
[37] M. Bösing, I. Loose, H. Pohlmann, B. Krebs, Chem. Eur. J. 3 (1997) 1232.
[38] I. Loose, E. Droste, M. Bösing, H. Pohlmann, M.H. Dickman, C. Rosu, M.T. Pope, B. Krebs, Inorg. Chem. 38 (1999) 2688.
[39] D. Laurencin, R. Villanneau, P. Herson, R. Thouvenot, Y. Jeannin, A. Proust, Chem. Commun. (2005) 5524.
[40] L.H. Bi, B. Li, L.X. Wu, J. Coord. Chem. 62 (2009) 531.
[41] L.H. Bi, B. Li, Y.Y. Bao, L.X. Wu, Inorg. Chem. Acta 362 (2009) 1600.
[42] A.A. Rachford, J.L. Petersen, J.J. Rack, Inorg. Chem. 44 (2005) 8065.
[43] I.D. Brown, D. Altermatt, Acta Cryst. B 41 (1985) 244.
[44] E. Alessio, G. Mestroni, G. Nardin, W.M. Attia, M. Calligaris, G. Sava, S. Zorzet, Inorg. Chem. 27 (1988) 4099.
[45] L.H. Bi, T. McCormac, S. Beloshapkin, E. Dempsey, Electroanalysis 20 (2008) 38.